Peoples Democratic Republic of Algeria
Ministry of Higher Education and Scientific Research Kasdi
Merbah University Ouargla
Faculty of Mathematics and Material Sciences
Department of Physics

MASTER THESIS

Domain: **Material Sciences**
Specialty: **Theoretical Physics**

Probing Gravitational Instability for Hernquist Potential

Presented by:

Zouaouid Zineb

Publicly defended on 17/05/2026 before the examination committee composed of:

Pr. Bentouila Omar	President	(Univ. Ouargla)
Dr. Zenkhri Djamel Eddine	Examiner	(Univ. Ouargla)
Dr. Benkrane Abdelhakim	Supervisor	(Univ. Ouargla)

Academic Year: 2025 / 2026

Acknowledgements

I would like to express my sincere gratitude and appreciation to my supervisor, Benkrane Abdelhakim, for his continuous support, valuable guidance, and great patience throughout the preparation of this dissertation. His scientific advice and encouragement had a significant impact on the completion of this work. I would also like to extend my heartfelt thanks and appreciation to the examining professors for accepting to evaluate this dissertation and for their valuable scientific remarks, which will undoubtedly contribute to enriching and improving this work. Furthermore, I would like to thank the Department of Physics at Kasdi Merbah University Ouargla, as well as all its staff members. May God bless them all and reward them abundantly for their efforts.

Dedication

To those who have been my support and strength throughout all stages of my life, to the dearest people to my heart, my beloved family, I dedicate this humble work in gratitude for their kindness, sacrifices, patience, and continuous encouragement. To my beloved parents, may God protect them, who instilled in me the love of knowledge and hard work, and who have always been a source of strength and hope. To my brothers, sisters, and all members of my family, thank you for your love and support, which motivated me to continue and achieve this accomplishment. I dedicate to you the fruit of this effort with all pride and affection.

Contents

Abstract

This thesis investigates gravitational instability in self-gravitating systems using Jeans analysis through both energetic and dynamical approaches. Several gravitational potentials are studied, including the Newtonian, Plummer, fractional gravity, and MOND models, in order to analyze their effects on the Jeans mass, Jeans length, dispersion relation, and growth rate.

The main original contribution of this work is the detailed study of the Hernquist potential, where its impact on gravitational instability is analyzed using both energetic and dynamical approaches, and the results are discussed in connection with astrophysical observations.

الملخص

تبحث هذه الأطروحة في عدم الاستقرار الجاذبي في الأنظمة ذاتية الجاذبية باستخدام تحليل جينز من خلال المقاربتين الطاقية والديناميكية. وقد تمت دراسة عدة جهود جاذبية، بما في ذلك نماذج نيوتن، بلامر، الجاذبية الكسرية وMOND وذلك لتحليل تأثيرها على كتلة جينز، وطول جينز، وعلاقة التشتت، ومعدل النمو.

تتمثل المساهمة الأصلية الرئيسية لهذا العمل في الدراسة التفصيلية لجهد هيرنكويست، حيث تم تحليل تأثيره على عدم الاستقرار الجاذبي باستخدام كلٍّ من المقاربتين الطاقية والديناميكية، كما تمت مناقشة النتائج وربطها بالمشاهدات الفيزيائية الفلكية.

Résumé

Ce mémoire porte sur l'étude de l'instabilité gravitationnelle dans les systèmes auto-gravitants à l'aide de l'analyse de Jeans selon les approches énergétique et dynamique. Plusieurs potentiels gravitationnels sont étudiés, notamment les potentiels newtonien, de Plummer, la gravité fractionnaire et MOND, afin d'analyser leurs effets sur la masse de Jeans, la longueur de Jeans, la relation de dispersion et le taux de croissance.

La principale contribution originale de ce travail est l'étude détaillée du potentiel de Hernquist, dont l'effet sur l'instabilité gravitationnelle est analysé à l'aide des deux approches, énergétique et dynamique, avec une comparaison aux observations astrophysiques.

General Introduction

The Jeans analysis is one of the fundamental pillars in astrophysics and cosmology, as it is used to study the stability of self-gravitating systems and to understand the physical conditions that lead to the collapse of gaseous clouds and the formation of cosmic structures such as stars and galaxies. This analysis is based on a key idea involving the competition between two main effects: thermal pressure, which tends to resist collapse, and self-gravity, which promotes clustering and contraction.

The Jeans analysis can be approached through two main methods. The first is the energetic approach, which relies on comparing the thermal kinetic energy with the gravitational potential energy, where collapse occurs when gravity overcomes pressure. The second is the dynamical approach, which is based on studying the evolution of small perturbations within the medium through a linear analysis of the hydrodynamic equations. This allows determining the perturbation frequency, growth rate, and distinguishing between stable and unstable systems.

Due to its importance, the Jeans analysis has received significant attention in the scientific literature and has been extended to more complex situations, such as inhomogeneous media, quantum effects, and modified gravity models. This theoretical framework is widely used to understand structure formation in the universe and to connect theoretical predictions with astrophysical observations.

In this work, we studied gravitational instability within this framework through three main stages:

In the first chapter, we adopted the energetic approach to study the Jeans criterion, analyzing the effect of different gravitational potentials (Newtonian, Plummer, fractional gravity, and MOND) on the Jeans mass and length.

In the second chapter, we moved to the dynamical approach using linear perturbation analysis, where we derived the dispersion relation and growth rate, and studied both the classical and quantum systems.

In the third chapter, we focused on the Hernquist potential, investigating the effect of the internal structure of the system (through a characteristic scale length) on gravitational instability, using both energetic and dynamical approaches, and linking the results to observational data.

Chapter 1

the Jeans Instability: Energy approach

1 Introduction

Jeans criterion determines when a gas cloud in space becomes gravitationally unstable and begins to collapse, potentially forming stars or stellar clusters [1, 2]. It represents the threshold between stability and gravitational collapse, depending on the clouds temperature and density [3, 2]. A cloud becomes unstable when its self-gravity overcomes internal thermal pressure.

The origin of this concept goes back to James Jeans, a British physicist and astronomer, who introduced what is now known as the Jeans analysis. His objective was to investigate the physical conditions under which diffuse gaseous clouds can collapse and give rise to star formation. To achieve this, he studied the evolution of small perturbations in an initially homogeneous and isotropic medium, using the fundamental equations of hydrodynamics coupled with gravity [4, 5]. This analysis showed that the stability of the cloud is governed by the competition between internal pressure, which resists collapse, and self-gravity, which enhances it.

According to the classical Jeans analysis, gravitational collapse occurs when the mass of the cloud exceeds a critical value known as **the Jeans mass** [1, 3], given by

$$M_J = \left(\frac{5k_BT}{G\mu m_p}\right)^{3/2}\left(\frac{3}{4\pi\rho}\right)^{1/2}, \tag{1.1}$$

where k_B is the Boltzmann constant, T the temperature, G is the gravitational constant, μ the mean molecular mass, ρ the density, and m_p the mass of a proton atom.

The corresponding **Jeans radius** is given by

$$R_J = \sqrt{\frac{15k_BT}{4\pi G\mu m_p\rho}}, \tag{1.2}$$

Despite its simplifying assumptions (homogeneous, non-rotating, and non-magnetic medium), the Jeans criterion provides a fundamental estimate of the conditions required for star formation in astrophysics. Over the years, it has become a cornerstone in astrophysics and cosmology, attracting considerable interest and extensive developments [6, 7]. Many researchers have extended this framework to more complex and realistic physical scenarios, including non-isothermal media, turbulent environments, and magnetized systems [8, 9]. In particular, significant attention has been devoted to studying modified or generalized gravitational interactions, where the standard Newtonian potential is replaced by alternative potentials, leading to non-trivial modifications of the instability criterion [10, 11].

The aim of this chapter is to examine how different gravitational interactions influence the Jeans mass and the Jeans length, and to assess their role in the onset of gravitational instability.

2 Jeans Radius and Mass under Different Gravitational Potentials

The objective of this section is to present the Jeans radius and Jeans mass for gas clouds under varying potential energies, providing a detailed insight into the gravitational instability of these clouds and their potential to form stars.

2.1 Newtonian Gravitatioanl Potential

In the Newtonian framework, the gravitational potential describes the attraction between two masses. For a spherically symmetric mass distribution, this potential is given by [12]:

$$\Phi(r) = -\frac{GM}{r}. \tag{1.3}$$

The gravitational binding energy U is defined as

$$U = -\int_0^M \frac{Gm}{r}\, dm. \tag{1.4}$$

We have

$$m = \frac{4}{3}\pi\rho r^3 \quad \Rightarrow \quad dm = 4\pi\rho r^2\,dr. \tag{1.5}$$

$$U = -\frac{16\pi^2 G\rho^2}{3}\int_0^R r^4\,dr. \tag{1.6}$$

We find

$$U = -\frac{16}{15}\pi^2 G\rho^2 R^5. \tag{1.7}$$

We substitute

$$\rho = \frac{3M}{4\pi R^3} \quad \Rightarrow \quad \rho^2 = \frac{9M^2}{16\pi^2 R^6}, \tag{1.8}$$

the gravitational binding energy becomes

$$U = -\frac{3}{5}\frac{GM^2}{R}. \tag{1.9}$$

In a stable system at equilibrium, the thermal kinetic energy approximately equals the absolute value of the gravitational potential energy, i.e., $K \approx |U|$. The kinetic energy is given by

$$K = \frac{3}{2}Nk_BT. \tag{1.10}$$

$$N = \frac{M}{\mu m_H}, \tag{1.11}$$

where N is the total number of particles within the cloud

$$\frac{3}{2}\frac{M}{\mu m_p}k_BT = \frac{3}{5}\frac{GM^2}{R}. \tag{1.12}$$

$$M = \frac{4}{3}\pi\rho R^3, \tag{1.13}$$

and solving for R , we find

$$R_J^2 = \frac{15k_BT}{4\pi G\mu m_p\rho}. \tag{1.14}$$

We obtain the Jeans radius as follows:

$$R_J = \sqrt{\frac{15k_BT}{4\pi G\mu m_p\rho}}. \tag{1.15}$$

The corresponding Jeans Mass is written as follows

$$M_J = \left(\frac{5k_BT}{G\mu m_p}\right)^{3/2}\left(\frac{3}{4\pi\rho}\right)^{1/2}. \tag{1.16}$$

2.2 Plummer Sphere Profile

The Plummer sphere potential, originally introduced as a simple model to describe the distribution of matter within globular star clusters [13], has proven to be a valuable tool in astrophysics. It is widely used to characterize stellar density profiles in dwarf galaxies and to model point particles in N-body simulations. The corresponding gravitational potential is given by [14]:

$$\Phi(r) = -\frac{Gm}{\sqrt{r^2 + r_0^2}}. \tag{1.17}$$

Where r_0 denotes the softening length. This formulation, commonly referred to in the literature as the Plummer potential [15, 16], ensures that the gravitational potential remains finite at $r = 0$ while effectively reducing unphysical strong two-body interactions. Consequently, it has become a standard tool in N-body simulations of galaxies, galaxy clusters, and large-scale structure formation [17, 18, 19].

To analyze the Jeans instability, it is essential to evaluate the gravitational binding energy U, which is defined as

$$U = -\int_0^M \Phi\, dm, \tag{1.18}$$

where for the Plummer sphere potential, we have

$$U = -\int_0^M \frac{Gm}{\sqrt{r^2 + r_0^2}}\, dm, \tag{1.19}$$

considering an idealized spherical cloud of radius R with uniform density ρ and total mass M, one finds

$$m(r) = \frac{4\pi}{3}\rho r^3 \quad \Rightarrow \quad dm = 4\pi\rho r^2\, dr. \tag{1.20}$$

$$M = \frac{4\pi}{3}\rho R^3. \tag{1.21}$$

Using Eqs. (1.20) and (1.21), the gravitational binding energy can be expressed as follows

$$U = -\frac{GM^2}{5R^6}\left(-8r_0^5 + \sqrt{R^2 + r_0^2}\left(3R^4 - 4R^2r_0^2 + 8r_0^4\right)\right). \tag{1.22}$$

In the limit $r_0 \to 0$, where the Plummer scale radius vanishes, the standard Newtonian expression for the binding energy is recovered.

$$U(r_0 = 0) = -\frac{3GM^2}{5R}. \tag{1.23}$$

For $r_0/R \ll 1$, the binding energy can be expanded in Eq. () up to second order in the small parameter r_0/R, yielding

$$U \simeq -\frac{3GM^2}{5R}\left(1 - \frac{5}{6}\left(\frac{r_0}{R}\right)^2\right). \tag{1.24}$$

The Jeans mass represents the minimum mass required for a gas cloud to become gravitationally unstable and undergo collapse. It can be estimated either by balancing the gravitational binding energy with the thermal kinetic energy or equivalently by applying the virial theorem. For a system in equilibrium, the thermal kinetic energy is approximately equal to the magnitude of the gravitational potential energy, i.e., $K \approx |U|$. The kinetic energy is expressed as follows.

$$K = \frac{3Nk_BT}{2} = \frac{3Mk_BT}{2m_p\mu}. \tag{1.25}$$

By inserting the expression for M from Eq. (1.21) into both the approximate binding energy (valid for $r_0/R \ll 1$, Eq. (1.23)) and the kinetic energy (Eq. (1.24)), it follows that, in the presence of a finite Plummer radius, gravitational collapse can only occur if the cloud radius exceeds a certain critical value.

$$R_J = \sqrt{\frac{15k_BT}{8G\pi m_p\mu\rho} + \frac{5r_0^2}{6}}, \tag{1.26}$$

which recovers the standard Jeans radius in the limit $r_0 \to 0$,

$$R_{J(r_0=0)} = \sqrt{\frac{15k_BT}{8G\pi m_p\mu\rho}}. \tag{1.27}$$

Once the Jeans radius is determined in the presence of r_0, the corresponding Jeans mass can be readily derived as follows:

$$M_J = \frac{4\pi\rho}{3}\left[\frac{15k_BT}{8G\pi m_p\mu\rho} + \frac{5r_0^2}{6}\right]^{3/2}. \tag{1.28}$$

This result indicates that a finite value of r_0 increases the critical mass required for gravitational collapse. Consequently, this effect may provide an explanation for interstellar clouds whose masses exceed the classical Jeans mass yet remain stable without collapsing. Furthermore, the parameter r_0 can be tuned to achieve consistency with observational data[13].

2.3 Fractional Gravitatioanl Potential

In the framework of fractional gravity, the gravitational potential due to a point mass m at position $\mathbf{r}$ can be expressed as [20]:

$$\Phi(r) = -\frac{\Gamma\left(\frac{3}{2}-s\right)}{4^{s-1}\sqrt{\pi}\Gamma(s)}\left(\frac{\ell}{\mathbf{r}}\right)^{2-2s}\frac{Gm}{\mathbf{r}}, \quad (1 \leq s < 3/2). \tag{1.29}$$

Here, Φ_s denotes the total gravitational potential in the fractional formulation, $\mathbf{r}$ is the position vector relative to the point mass, G is the universal gravitational constant, ℓ is a characteristic length associated with the fractional scale of gravity, and s is the fractional index that determines the deviation from the classical Newtonian gravity. The range of s is $1 \leq s < 3/2$, with the classical Newtonian case recovered at $s = 1$.

The gravitational potential energy is given by [12],

$$|U| = \frac{3\,\Gamma\left(\frac{3}{2}-s\right)}{4^{\,s-1}\sqrt{\pi}\,(3+2s)\,\Gamma(s)}\left(\frac{\ell}{R}\right)^{2-2s}\frac{GM^2}{R}, \tag{1.30}$$

where R denotes the radius of the spherical cloud. In the limit $s \to 1$, Eq. (1.29) recovers the standard expression $|U| = \frac{3GM^2}{5R}$. Meanwhile, the mean kinetic energy of the gas cloud is given by:

$$K = \frac{3Nk_BT}{2} = \frac{3MR_gT}{2\mu}, \tag{1.31}$$

where μ represents the mean molecular weight per particle, k_B denotes the Boltzmann constant, and $R_g \equiv \frac{k_B}{m_p}$. For a system in equilibrium, the kinetic energy is approximately equal to the magnitude of its potential energy, i.e.,

$$K = |U|.$$

However, when gravitational attraction overcomes the outward pressure, the system departs from equilibrium, triggering gravitational collapse. This instability sets in when $|U| > K$. By combining Eqs. (1.29) and (1.30), it follows that collapse occurs only if the cloud radius exceeds a critical threshold.

$$R_J^s = \left[\frac{2\,\Gamma\left(\frac{3}{2}-s\right)\,\mu GM}{(3+2s)\,4^{\,s-1}\sqrt{\pi}\,\Gamma(s)\,R_gT}\right]^{1/(3-2s)}. \tag{1.32}$$

By expressing the radius in terms of the density ρ_0, the Jeans mass can be written as follows:

$$M_J^s = \left[\left(\frac{3}{4\pi\rho_0} \right)^{1-\frac{2s}{3}} \frac{(3+2s)\,4^{s-1}\sqrt{\pi}\,\Gamma(s)\,R_g T}{\mu G\,\Gamma(3-2s)\,\ell^{2-2s}} \right]^{\frac{3}{2s}}. \tag{1.33}$$

It is worth noting that the critical mass in Eq. (1.32) exhibits a temperature dependence of the form $M_J^s \sim T^{3/2s}$ and a density dependence $M_J^s \sim \rho_0^{1-3/2s}$. In the limit $s \to 1$, the standard scaling relations $M_J \sim T^{3/2}$ and $M_J \sim \rho_0^{-1/2}$ are recovered. Under the same limit, the critical radius in Eq. (1.31) and the mass in Eq. (1.32) reduce to the classical Jeans length and Jeans mass, respectively [12]:

$$R_J = \frac{2GMu}{5R_gT}, \quad M_J = \left(\frac{5R_gT}{4\mu G} \right)^{3/2} \left(\frac{4}{3}\pi\rho_0 \right)^{-1/2}. \tag{1.34}$$

2.4 Modified Newton dynamics (MOND) $s = 3/2$

The gravitational potential of a spherical mass M at a distance r in the framework of fractional gravity is given by the following expression, which accounts for both the case $1 \leq s < 3/2$ and the special case $s = 3/2$:

$$\Phi(r) = \begin{cases} \dfrac{\Gamma\left(\frac{3}{2}-s\right)}{4^{s-1}\sqrt{\pi}\,\Gamma(s)} \left(\dfrac{\ell}{r}\right)^{2-2s} \dfrac{GM}{r}, & 1 \leq s < \frac{3}{2}. \\[2ex] \dfrac{2GM}{\pi\ell} \ln\left(\dfrac{r}{\ell}\right), & s = \frac{3}{2}. \end{cases} \tag{1.35}$$

In order to compute the gravitational binding energy, the expression of U is required, which is given as [21],

$$|U| = \int_0^M \Phi_{3/2}(r)\,dm. \tag{1.36}$$

Where for $\Phi_{3/2}(r)$, we have

$$|U| = \int_0^M \frac{2\pi Gm}{\ell} \ln\frac{r}{\ell}\,dm. \tag{1.37}$$

Consider an ideal spherical cloud of radius R, uniform density ρ, and total mass M, for which the following relations hold:

$$m(r) = \frac{4\pi}{3}\rho r^3 \quad \Rightarrow \quad dm = 4\pi\rho r^2 dr, \tag{1.38}$$

and

$$M = \frac{4\pi}{3}\rho R^3. \tag{1.39}$$

Using Eqs. (1.38) and (1.39), it is easy to show that

$$|U| = \frac{GM^2}{36\pi\ell}\left|6\ln\left(\frac{R}{\ell}\right) - 1\right|. \tag{1.40}$$

For a system in stable equilibrium, the thermal kinetic energy is approximately equal to the magnitude of the gravitational potential energy, i.e., $K = |U|$, where the kinetic energy is expressed as:

$$K = \frac{3Nk_BT}{2} = \frac{3Mk_BT}{2m_p\mu}. \tag{1.41}$$

By using Eqs. (13) and (14), it can be shown that gravitational collapse occurs only when the cloud radius exceeds a critical value.

$$R_J^{(s=\frac{3}{2})} = \ell\exp\left(\frac{W\left(\frac{A}{2\sqrt{e}}\right)}{3} + \frac{1}{6}\right), \tag{1.42}$$

where A is a dimensionless constant defined as follows:

$$A = \frac{81k_BT}{2Gm_p\rho\mu\ell^2}, \tag{1.43}$$

and $W(x)$ denotes the product logarithm (Lambert W function), defined as the solution of an equation of the form

$$x = \omega\exp(\omega). \tag{1.44}$$

Consequently, the Jeans mass is given by:

$$M_J^{(s=3/2)} = \frac{4\pi\rho\,\ell^3}{3}\exp\left[W\left(\frac{A}{2\sqrt{e}}\right) + \frac{1}{2}\right]. \tag{1.45}$$

The following table provides a concise summary of the key results for the Jeans radius and Jeans mass under various gravitational potentials, along with a direct comparison to the Newtonian case.

Potential	**Jeans Radius** R_J	**Jeans Mass** M_J	**Compared with Newtonian gravity**
Newtonian	$R_J = \sqrt{\frac{15k_BT}{4\pi G\mu m_p\rho}}$	$M_J = \left(\frac{5k_BT}{G\mu m_p}\right)^{3/2}\left(\frac{3}{4\pi\rho}\right)^{1/2}$	Reference timescale
Plummer	$R_J = \sqrt{\frac{15k_BT}{8\pi Gm_p\mu\rho} + \frac{5r_0^2}{6}}$	$M_J = \frac{4\pi\rho}{3}\left(\frac{15k_BT}{8\pi Gm_p\mu\rho} + \frac{5r_0^2}{6}\right)^{3/2}$	Slower than Newtonian
Fractional $1 \leq s < \frac{3}{2}$	$R_J = \left[\frac{2\Gamma(\frac{3}{2}-s)\mu GM}{(3+2s)4^{s-1}\sqrt{\pi}\Gamma(s)R_gT}\right]^{1/(3-2s)}$	$M_J = \left(\frac{3}{4\pi\rho_0}\right)^{1-\frac{2s}{3}} \times \left[\frac{(3+2s)4^{s-1}\sqrt{\pi}\Gamma(s)R_gT}{\mu G\Gamma(3-2s)\ell^{2-2s}}\right]^{\frac{3}{2s}}$	Depends on s
MOND $(s = \frac{3}{2})$	$R_J = \ell \exp\left(\frac{W\left(\frac{A}{2\sqrt{e}}\right)}{3} + \frac{1}{6}\right)$	$M_J = \frac{4\pi\rho}{3}\ell^3 \exp\left(W\left(\frac{A}{2\sqrt{e}}\right) + \frac{1}{2}\right)$	Depends on Lambert W

Table 1.1: Comparison of Jeans radius and Jeans mass for different gravitational potentials

3 Conclusion

In this chapter, we studied the Jeans gravitational instability for a set of different gravitational potentials, including the Newtonian gravitational potential, the Plummer sphere profile, and the fractional gravitational potential. This analysis allowed us to determine how each potential affects the calculation of the Jeans mass and Jeans radius, which are the fundamental parameters that govern the collapse conditions of gaseous clouds. Thus, everything addressed in this study contributes to a deeper understanding of the mechanisms of star formation in various physical environments and clarifies how changes in the form of the gravitational potential lead to significant diversity in the resulting stellar structures. Although the results obtained in this chapter are essential for understanding the threshold at which collapse begins, they remain limited, as they do not provide information about the time evolution of perturbations, their growth rate, or how to distinguish between dynamically stable and unstable states. This limitation constitutes a direct motivation for moving to the next level of analysis. Therefore, the discussion presented in this chapter establishes the theoretical foundation and necessary reference for the second chapter, where we will move from an approach based on the comparison of kinetic energy and gravitational potential energy to a more comprehensive and accurate linear dynamical treatment.

Chapter 2

Linear Analysis of Jeans Instability: Dynamical Approach

1 Introduction

In this chapter, we examine the stability of self-gravitating clouds by analyzing **small deviations from a homogeneous gaseous medium**. These deviations, known as perturbations, represent localized regions of density or velocity that differ slightly from the average values of the medium. Studying such perturbations allows us to determine whether small fluctuations will *oscillate, remain steady, or grow over time*, providing insight into the conditions under which gravitational collapse may occur [1, 22]. To quantify this behavior, small perturbations in density and velocity are introduced into a uniform medium characterized by background density ρ_0 and sound speed c_s. The evolution of these perturbations is governed by the **dispersion relation**

$$\omega^2 = c_s^2 k^2 - 4\pi G\rho_0, \tag{2.1}$$

which distinguishes between *stable modes* ($\omega^2 > 0$), oscillating with frequency ω, and *unstable modes* ($\omega^2 < 0$), which grow exponentially at a rate

$$\gamma = \sqrt{4\pi G\rho_0 - c_s^2 k^2}. \tag{2.2}$$

The marginally stable mode occurs at the critical wavenumber $k = k_J$, where perturbations evolve linearly in time [23, 24]. This approach provides a clear **dynamical perspective** on the onset of gravitational collapse and complements other methods for studying structure formation

[25, 26]. It is widely used in astrophysics to describe the formation of molecular clouds and the early stages of star formation [27, 28]. The dispersion relation has attracted considerable attention in the scientific community due to its fundamental role in understanding the evolution of perturbations in physical media, particularly in self-gravitating systems. Many studies have also extended this framework to different gravitational potentials, including modified models, in order to investigate their impact on stability criteria and growth rates [29, 30, 24].

2 Hydrodynamic Approach

2.1 Classical Regime

Beyond merely comparing kinetic and gravitational binding energies, the Jeans mechanism is more clearly understood from a hydrodynamic viewpoint [31], which enables the analysis of the growth rates of perturbations. At the fluid level of description, the dynamics of the medium is governed by the continuity equation

$$\frac{\partial \rho}{\partial t} + \nabla \cdot (\rho \mathbf{u}) = 0. \tag{2.3}$$

The continuity equation ensures mass conservation in a fluid, stating that the local change in density equals the net mass flux across the boundary. where $\frac{\partial \rho}{\partial t}$ is the local (temporal) rate of change of density, and $\nabla \cdot (\rho \mathbf{u})$ is the divergence of the mass flux, representing the net flow of mass into or out of a small volume. $\rho(\mathbf{r}, t)$ denotes the mass density and $\mathbf{u}(\mathbf{r}, t)$ is the velocity field. The momentum balance is described by the Euler equation,

$$\frac{\partial \mathbf{u}}{\partial t} + (\mathbf{u} \cdot \nabla)\mathbf{u} = -\nabla \Phi - \frac{1}{\rho} \nabla p. \tag{2.4}$$

The Euler equation describes the motion of an ideal (inviscid) fluid and represents the application of Newtons second law to a differential fluid element. $\frac{\partial \mathbf{u}}{\partial t}$ is the local (temporal) acceleration, $(\mathbf{u} \cdot \nabla)\mathbf{u}$ is the convective acceleration, p is the pressure, ρ is the fluid density, $-\frac{1}{\rho}\nabla p$ represents the pressure force per unit mass, $-\nabla\Phi$ represents the external force derived from the potential field, Φ is the self-gravitational potential, which is related to the density through the Poisson equation.

$$\nabla^2 \Phi(\vec{r}) = 4\pi G \rho(\vec{r}). \tag{2.5}$$

We consider a general barotropic fluid (i.e. a fluid in which the pressure is uniquely determined by the local mass density and does not depend explicitly on temperature or entropy), for which the pressure is a function of the mass density alone, namely

$$p(\mathbf{r},t) = p[\rho(\mathbf{r},t)]\,. \tag{2.6}$$

we substitute the density coefficient into the equation (2.3) and (2.3):

$$\nabla\cdot(\rho\vec{u}\otimes\vec{u}) = \rho(\vec{u}\cdot\nabla)\vec{u} + \vec{u}\,(\nabla\cdot(\rho\vec{u}))\,, \tag{2.7}$$

$$\frac{\partial}{\partial t}(\rho\vec{u}) + \nabla\cdot(\rho\vec{u}\otimes\vec{u}) = \rho\frac{\partial\vec{u}}{\partial t} + \rho(\vec{u}\cdot\nabla)\vec{u} + \vec{u}\left(\frac{\partial\rho}{\partial t} + \nabla\cdot(\rho\vec{u})\right). \tag{2.8}$$

Using the continuity equation:

$$\frac{\partial\rho}{\partial t} + \nabla\cdot(\rho\vec{u}) = 0, \tag{2.9}$$

$$\rho\frac{\partial\vec{u}}{\partial t} + \rho(\vec{u}\cdot\nabla)\vec{u} = -\nabla p - \rho\nabla\Phi. \tag{2.10}$$

Dividing both sides by ρ , we obtain :

$$\frac{\partial\vec{u}}{\partial t} + (\vec{u}\cdot\nabla)\vec{u} = -\frac{1}{\rho}\nabla p - \nabla\Phi, \tag{2.11}$$

we use Green's functions

$$\nabla^2 G(\mathbf{r},\mathbf{r}') = \delta(\mathbf{r}-\mathbf{r}'), \tag{2.12}$$

the gravitational potential can be written as:

$$\Phi(\mathbf{r}) = -G\int\frac{\rho(\mathbf{r}')}{|\mathbf{r}-\mathbf{r}'|}\,d\mathbf{r}', \tag{2.13}$$

$$\Phi(\mathbf{r}) = \frac{1}{m}\int\rho(\mathbf{r}')\,\Phi(\mathbf{r}-\mathbf{r}')\,d\mathbf{r}', \tag{2.14}$$

we obtain the following equation:

$$\frac{\partial\vec{u}}{\partial t} + (\vec{u}\cdot\nabla)\vec{u} = -\nabla\left[\frac{1}{m}\int\rho(\mathbf{r}')\,\Phi(\mathbf{r}-\mathbf{r}')\,d\mathbf{r}'\right] - \frac{\nabla p}{\rho}. \tag{2.15}$$

We restrict our analysis to the linear regime by considering small perturbations about a stationary, infinite, homogeneous, and an isotropic equilibrium background. For a stationary medium

($\mathbf{u}_0 = 0$), the density and velocity fields can be written as

$$\rho(\mathbf{r}, t) = \rho_0 + \delta\rho(\mathbf{r}, t), \qquad \mathbf{u}(\mathbf{r}, t) = \delta\mathbf{u}(\mathbf{r}, t). \tag{2.16}$$

where $\delta\rho$ and $\delta\mathbf{u}$ are assumed to be small perturbations. By linearizing the fluid equations (2.6) and (2.3), we obtain

$$\frac{\partial\, \delta\rho(\mathbf{r}, t)}{\partial t} + \rho_0 \nabla \cdot \delta\mathbf{u}(\mathbf{r}, t) = 0, \tag{2.17}$$

$$\frac{\partial\, \delta\mathbf{u}(\mathbf{r}, t)}{\partial t} = -\nabla \left[\frac{1}{m} \int \delta\rho(\mathbf{r}', t) \Phi |\mathbf{r} - \mathbf{r}'|\, d\mathbf{r}' \right] - \frac{c_s^2}{\rho_0} \nabla \delta\rho(\mathbf{r}, t), \tag{2.18}$$

where

$$C_s^2 = \left(\frac{dP}{d\rho} \right)_{\rho=\rho_0}$$

we assume that small perturbations in density and velocity propagate as plane waves:

$$\delta\rho(\mathbf{r}, t) = \delta\rho_k e^{i(\mathbf{k}\cdot\mathbf{r} - \omega t)}, \qquad \delta\mathbf{u}(\mathbf{r}, t) = \delta\mathbf{u}_k e^{i(\mathbf{k}\cdot\mathbf{r} - \omega t)} \tag{2.19}$$

Thus, in Fourier space, the differential operators become:

$$\frac{\partial}{\partial t} \to -i\omega, \qquad \nabla \to i\mathbf{k} \tag{2.20}$$

Fourier transform of the continuity equation (2.17)

$$-i\omega\delta\rho_k + i\rho_0(\mathbf{k} \cdot \delta\mathbf{u}_k) = 0 \tag{2.21}$$

which gives:

$$\mathbf{k} \cdot \delta\mathbf{u}_k = \frac{\omega}{\rho_0} \delta\rho_k \tag{2.22}$$

Fourier transform of the momentum equation (2.18)

$$\frac{\partial \delta\mathbf{u}}{\partial t} = -\nabla \left[\frac{1}{m} \int \delta\rho(\mathbf{r}') \Phi(\mathbf{r} - \mathbf{r}')\, d\mathbf{r}' \right] - \frac{c_s^2}{\rho_0} \nabla \delta\rho. \tag{2.23}$$

In the following, we will show what is the Fourier transform of the term$\int \delta\rho(\mathbf{r}')\Phi(\mathbf{r} - \mathbf{r}')\, d\mathbf{r}'$

$$f(\mathbf{r}) = \int \delta\rho(\mathbf{r}')\, \Phi(\mathbf{r} - \mathbf{r}')\, d\mathbf{r}'. \tag{2.24}$$

By definition, the Fourier transform of a function $g(\mathbf{r})$ is

$$\tilde{g}(\mathbf{k}) = \int g(\mathbf{r})\, e^{-i\mathbf{k}\cdot\mathbf{r}}\, d\mathbf{r}. \tag{2.25}$$

We now compute the Fourier transform of $f(\mathbf{r})$:

$$\tilde{f}(\mathbf{k}) = \int f(\mathbf{r})\, e^{-i\mathbf{k}\cdot\mathbf{r}}\, d\mathbf{r} \tag{2.26}$$

$$= \int \left[\int \delta\rho(\mathbf{r}')\, \Phi(\mathbf{r}-\mathbf{r}')\, d\mathbf{r}' \right] e^{-i\mathbf{k}\cdot\mathbf{r}}\, d\mathbf{r}. \tag{2.27}$$

Interchanging the order of integration gives

$$\tilde{f}(\mathbf{k}) = \int \delta\rho(\mathbf{r}') \left[\int \Phi(\mathbf{r}-\mathbf{r}')\, e^{-i\mathbf{k}\cdot\mathbf{r}}\, d\mathbf{r} \right] d\mathbf{r}'. \tag{2.28}$$

Now perform the change of variable

$$\mathbf{R} = \mathbf{r} - \mathbf{r}', \qquad \mathbf{r} = \mathbf{R} + \mathbf{r}', \qquad d\mathbf{r} = d\mathbf{R}.$$

Then

$$\int \Phi(\mathbf{r}-\mathbf{r}')\, e^{-i\mathbf{k}\cdot\mathbf{r}}\, d\mathbf{r} = \int \Phi(\mathbf{R})\, e^{-i\mathbf{k}\cdot(\mathbf{R}+\mathbf{r}')}\, d\mathbf{R} \tag{2.29}$$

$$= e^{-i\mathbf{k}\cdot\mathbf{r}'} \int \Phi(\mathbf{R})\, e^{-i\mathbf{k}\cdot\mathbf{R}}\, d\mathbf{R}. \tag{2.30}$$

The remaining integral is precisely the Fourier transform $\tilde{\Phi}(\mathbf{k})$, hence

$$\int \Phi(\mathbf{r}-\mathbf{r}')\, e^{-i\mathbf{k}\cdot\mathbf{r}}\, d\mathbf{r} = e^{-i\mathbf{k}\cdot\mathbf{r}'}\tilde{\Phi}(\mathbf{k}). \tag{2.31}$$

Substituting back,

$$\tilde{f}(\mathbf{k}) = \tilde{\Phi}(\mathbf{k}) \int \delta\rho(\mathbf{r}')\, e^{-i\mathbf{k}\cdot\mathbf{r}'}\, d\mathbf{r}' \tag{2.32}$$

$$= \tilde{\Phi}(\mathbf{k})\, \delta\tilde{\rho}(\mathbf{k}). \tag{2.33}$$

Therefore,

$$\boxed{\mathcal{F}[\delta\rho * \Phi] = \ \delta\tilde{\rho}(\mathbf{k}).\, \tilde{\Phi}(\mathbf{k})} \tag{2.34}$$

which proves that convolution in real space becomes multiplication in Fourier space. Therefore, one obtains:

$$-i\omega\delta\mathbf{u}_k = -i\mathbf{k}\,\delta\tilde{\rho}(\mathbf{k}).\left(\frac{\tilde{\Phi}(\mathbf{k})}{m} + \frac{c_s^2}{\rho_0}\right). \tag{2.35}$$

Taking the scalar product with $\mathbf{k}$, we have:

$$\mathbf{k}\cdot\delta\mathbf{u}_k = \frac{k^2}{\omega}\,\delta\rho(\mathbf{k}).\left(\frac{\tilde{\Phi}(\mathbf{k})}{m} + \frac{c_s^2}{\rho_0}\right). \tag{2.36}$$

Using the result from the continuity equation:

$$\frac{\omega}{\rho_0}\,\delta\tilde{\rho}(\mathbf{k}) = \frac{k^2}{\omega}\,\delta\tilde{\rho}(\mathbf{k}).\left(\frac{\tilde{\Phi}(\mathbf{k})}{m} + \frac{c_s^2}{\rho_0}\right). \tag{2.37}$$

Multiply Eq. (2.37) by ω, one arrives at the following dispersion relation:

$$\omega^2 = \frac{\rho_0}{m}\tilde{\Phi}(k)k^2 + c_s^2k^2, \tag{2.38}$$

where

$$\tilde{\Phi}(k) = \int \Phi(r)\,e^{-i\mathbf{k}\cdot\mathbf{r}}\,d\mathbf{r}, \tag{2.39}$$

is the Fourier transform of the self-potential $\Phi(r)$. Instabilities are indicated by the presence of an imaginary component in the mode frequency. We therefore decompose the frequency as

$$\omega = \omega_r + i\,\omega_i. \tag{2.40}$$

Since ω^2 is real, the frequency must be either purely real or purely imaginary. The marginal case $\omega = 0$ defines a critical wavenumber that separates these two regimes. According to the dispersion relation (2.38), this critical wavenumber k_J is the solution of the following equation

$$\frac{\rho_0}{m}\tilde{\Phi}(k_J) + c_s^2 = 0. \tag{2.41}$$

The Jeans wavenumber k_J is related to the Jeans wavelength λ_J as follows [32]:

$$k = \frac{2\pi}{\lambda}. \tag{2.42}$$

For $k > k_J$ ($\lambda < \lambda_J$), the frequency takes the form $\omega = \omega_r = \pm\sqrt{\omega^2}$, implying that the perturbation evolves as $\sim \exp(-i\omega_r t)$ with a real frequency

$$\omega_r = \sqrt{\frac{\rho_0}{m}\tilde{\Phi}(k)k^2 + c_s^2 k^2}, \tag{2.43}$$

and therefore propagates without damping. This regime corresponds to gravity-modified acoustic waves, for which the system remains stable. In contrast, for $k < k_J$, the frequency becomes purely imaginary, $\omega = \omega_i = \gamma == \pm i\sqrt{-\omega^2}$, leading to a non-oscillatory exponential growth of the perturbation, $\sim \exp(\omega_i t)$. The associated growth rate is given by

$$\gamma = \sqrt{-\tilde{\Phi}(k)k^2 - c_s^2 k^2}. \tag{2.44}$$

In this case, the system is unstable and undergoes a gravitational collapse [13].

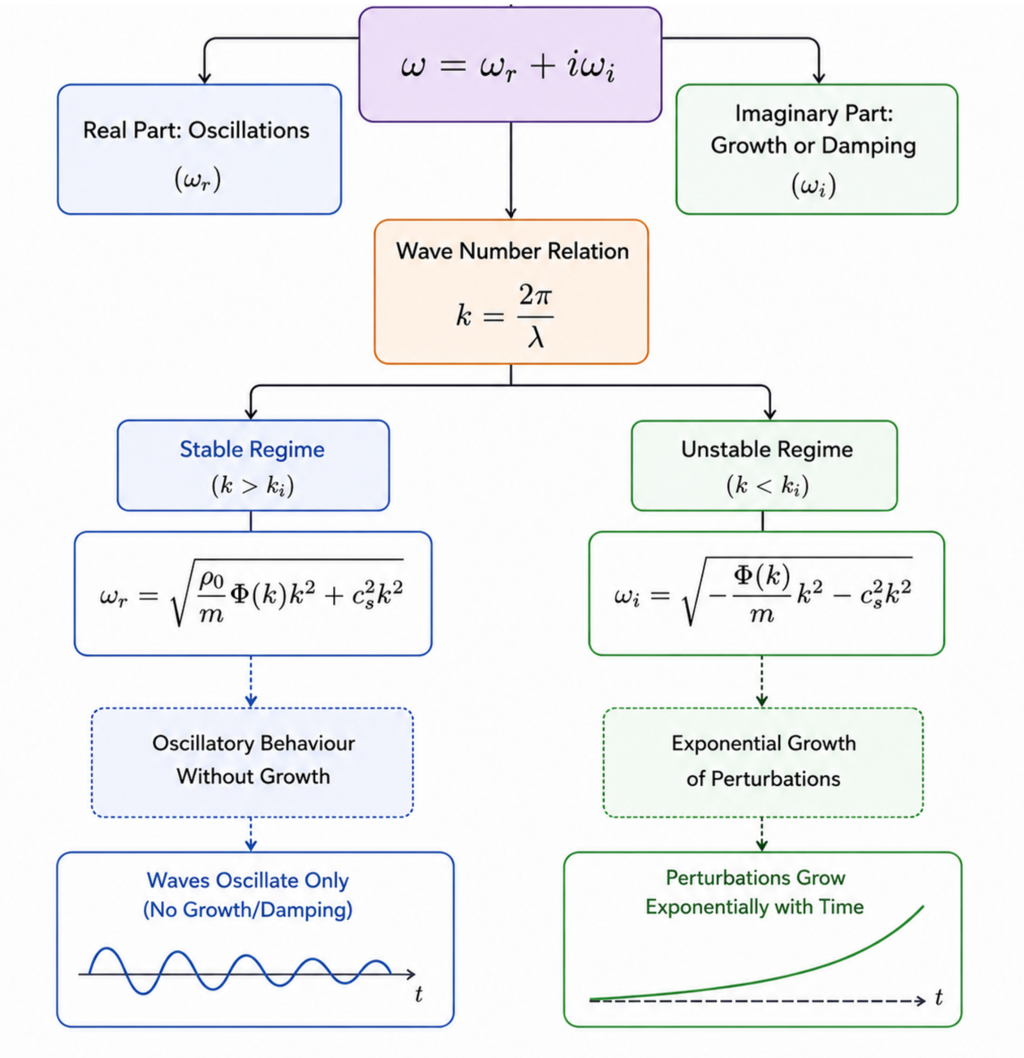

Figure 2.1: Perturbation Frequency and Gravitational Instability and Stability: A Jeans Analysis

Although this analysis has been carried out withinthe framework of a static universesufficient for establishing the stability criterionthe extension to an expanding background is straightforward (see, e.g. [33]). In this setting, the density contrast, defined as $\delta(t) := \delta\rho(t)/\rho_0$, obeys

$$\ddot{\delta} + 2\frac{\dot{a}_{\rm s}}{a_{\rm s}}\dot{\delta} + \left[\frac{c_s^2 k^2}{a^2} + \frac{\rho_0}{m}\left(\frac{k}{a_{\rm s}}\right)^2 \tilde{\Phi}\left(\frac{k}{a_{\rm s}}\right)\right]\delta = 0. \tag{2.45}$$

Here, $a(t)$ denotes the scale factor. This equation can be viewed as a natural extension of Bonnor's equation [33] to the framework of fractional gravity. In the static limit ($a = 1$), the dispersion relation (2.38) is recovered by assuming $\delta \propto e^{-i\omega t}$.

2.2 Quantum Regime

Classical analyses of gravitational instability account for pressure as the primary mechanism opposing collapse. In physical regimes characterized by low temperatures, high densities, or very light particlessuch as the early universe, compact astrophysical objects, or certain dark matter scenariosquantum effects become non-negligible and can significantly modify the stability properties of the system. In such contexts, wave-like behavior and quantum pressure must be incorporated into the description of self-gravitating matter. A convenient semiclassical framework for treating gravitational instability in the quantum regime is provided by the Schrödinger–Newton (or Schrödinger–Poisson) system. Originally formulated by Ruffini and Bonazzola in their study of boson stars [34], this model establishes a coupling between a quantum wave function and a classical gravitational field. Later, Díosi and Penrose [35, 36] explored the same structure as a possible phenomenological mechanism for gravity-induced wavefunction collapse. Within this approach, the wave function $\psi(\mathbf{r}, t)$ evolves according to

$$i\hbar\frac{\partial\psi}{\partial t} = -\frac{\hbar^2}{2m}\nabla^2\psi + m\Phi\psi, \tag{2.46}$$

$$\nabla^2\Phi = 4\pi G m|\psi|^2, \tag{2.47}$$

where the mass density sourcing the gravitational field is $\rho = m|\psi|^2$. Eliminating Φ leads to an integro–differential representation,

$$i\hbar\frac{\partial\psi}{\partial t} = -\frac{\hbar^2}{2m}\nabla^2\psi - m\int \Phi(|\mathbf{r}-\mathbf{r}'|)|\psi(\mathbf{r}',t)|^2\, d^3\mathbf{r}'\,\psi(\mathbf{r},t). \tag{2.48}$$

To establish a direct analogy with fluid dynamics, we employ the Madelung transformation [37], expressing the wave function in polar form,

$$\psi(\mathbf{r},t) = A(\mathbf{r},t)\, e^{iS(\mathbf{r},t)/\hbar}. \tag{2.49}$$

Here A and S denote the amplitude and phase, respectively, with

$$\rho(\mathbf{r},t) = |\psi|^2 = A^2(\mathbf{r},t), \tag{2.50}$$

defining the mass density. The associated velocity field is introduced through

$$\mathbf{u} = \frac{\nabla S}{m}. \tag{2.51}$$

Substituting Eq. (2.49) into Eq. (2.48) and separating real and imaginary parts yields a pair of hydrodynamic-type equations. The imaginary component produces the continuity equation,

$$\frac{\partial \rho}{\partial t} + \nabla \cdot (\rho \mathbf{u}) = 0, \tag{2.52}$$

while the real component leads to a quantum Hamilton–Jacobi equation,

$$\frac{\partial S}{\partial t} + \frac{(\nabla S)^2}{2m} + \int \rho(\mathbf{r}',t)\Phi(|\mathbf{r}-\mathbf{r}'|)d^3\mathbf{r}' + Q = 0, \tag{2.53}$$

where the quantum (Bohm) potential is given by

$$Q = -\frac{\hbar^2}{2m}\frac{\nabla^2 A}{A} = -\frac{\hbar^2}{4m}\left[\frac{\nabla^2 \rho}{\rho} - \frac{1}{2}\left(\frac{\nabla \rho}{\rho}\right)^2\right]. \tag{2.54}$$

Taking the gradient of the Hamilton–Jacobi equation and dividing by m yields the quantum analogue of the Euler equation,

$$\frac{\partial \mathbf{u}}{\partial t} + (\mathbf{u}\cdot\nabla)\mathbf{u} = -\nabla \int \rho(\mathbf{r}',t)V(|\mathbf{r}-\mathbf{r}'|)d^3\mathbf{r}' - \frac{1}{m}\nabla Q, \tag{2.55}$$

with $V(r) = \Phi(r)/m$. The continuity equation together with the above momentum equation form the quantum counterpart of the classical fluid system. Proceeding as in the classical analysis, we linearize around a homogeneous, stationary configuration with density ρ_0 and vanishing velocity. Introducing small perturbations and performing a Fourier decomposition leads to the dispersion relation

$$\omega'^2 = \rho_0 \tilde{V}(k) k^2 + \frac{\hbar^2 k^4}{4m^2}. \tag{2.56}$$

Equation (2.56) reveals the competition between self-gravity and quantum effects. In contrast to the classical pressure contribution, which scales as k^2, the quantum correction introduces a higher-order term proportional to k^4. This term becomes dominant at sufficiently short wavelengths and acts to suppress gravitational collapse in that regime..

3 Special Cases

3.1 Newtonian Gravitatioanl Potential

For this gravity potential, the Fourier transform is written as [12],

$$\tilde{\Phi}(k)_{\text{Newton}} = -GM \int \frac{e^{-i\mathbf{k}\cdot\mathbf{r}}}{r} d\mathbf{r}. \tag{2.57}$$

It is well-known that the Newtonian potential satisfies

$$\nabla \left(\frac{1}{|\mathbf{r}|} \right) = -4\pi\delta(\mathbf{r}). \tag{2.58}$$

Now take the Fourier transform of both sides

$$\nabla^2 \to -k^2, \tag{2.59}$$

$$\delta(\mathbf{r}) \to 1, \tag{2.60}$$

therefore,

$$-k^2 \tilde{V}(k) = -4\pi \Rightarrow \tilde{V}(k) = \frac{4\pi}{k^2}, \tag{2.61}$$

on other side, the Fourier transform of the Newton potential is written as

$$\tilde{\Phi}(k)_{\text{Newton}} = -\frac{4\pi GM}{k^2}. \tag{2.62}$$

In this case, the classical dispersion relation becomes

$$\omega^2 = -4\pi G\rho_0 + c_s^2 k^2. \tag{2.63}$$

As a result, the Jeans wave number for Newtonian gravity is written as

$$k_J = \frac{\Omega_J}{c_s}, \tag{2.64}$$

where $\Omega_J = \sqrt{4\pi G\rho_0}$ is the Jeans frequency [12]. In this case, the growth rate is written as follows

$$\gamma = \sqrt{\Omega_J^2 - c_s^2 k^2}. \tag{2.65}$$

We next consider the quantum regime. In this framework, the dispersion relation is modified by the inclusion of the quantum pressure term, yielding [12],

$$\omega'^2 = -\Omega_J^2 + \frac{\hbar^2 k^4}{4m^2}. \tag{2.66}$$

The instability occurs when $\omega^2 < 0$, leading to an exponential growth of perturbations. The corresponding growth rate is given by:

$$\gamma' = \sqrt{\Omega_J^2 - \frac{\hbar^2 k^4}{4m^2}}. \tag{2.67}$$

This expression shows that quantum effects introduce a stabilizing contribution at high wavenumbers, suppressing gravitational collapse at small scales [12].

3.2 Plummer Sphere Profile

In the classical regime, the potential expression is given by Eq. (1.17). Using the results obtained in ref.[13], the generic dispersion relation is written as

$$\omega^2 = -\Omega_J^2 k r_0 K_1(r_0 k) + c_s^2 k^2, \tag{2.68}$$

$K_\alpha(x)$ is the modified Bessel function of the second kind. For this potential, the Jeans wavenumber $k_J^{(r_0)}$ verifies

$$K_1(r_0 k_J^{(r_0)}) = \frac{c_s^2 k_J^{(r_0)}}{r_0 \Omega_J^2}. \tag{2.69}$$

for $k > k_J$, the perturbations oscillate with a real frequency given by

$$\omega_r = \sqrt{c_s^2 k^2 - \Omega_J^2\, kr_0 K_1(kr_0)}. \tag{2.70}$$

Conversely, for $k < k_J$, the perturbations become gravitationally unstable and grow exponentially with a growth rate

$$\gamma = \sqrt{\Omega_J^2\, kr_0 K_1(kr_0) - c_s^2 k^2}. \tag{2.71}$$

In the paper [13] , the author showed that the Plummer sphere exhibits a reduced growth rate compared to standard Newtonian gravity. Both cases reach their maximum growth rate at zero wavenumber; however, incorporating the Plummer radius r_0 shifts the critical wavenumberwhere the growth rate drops to zerotoward smaller values. The present results therefore indicate that introducing a softening length causes gravitational instability to favor larger wavelength perturbations relative to the classical Newtonian scenario . In the case of the Plummer potential, the inclusion of quantum effects leads to the following dispersion relation [13],

$$\omega'^2 = -\Omega_J^2\, kr_0 K_1(kr_0) + \frac{\hbar^2 k^4}{4m^2}. \tag{2.72}$$

The associated growth rate is given by:

$$\gamma' = \sqrt{\Omega_J^2\, kr_0 K_1(kr_0) - \frac{\hbar^2 k^4}{4m^2}}. \tag{2.73}$$

The presence of the scale parameter r_0 modifies the gravitational term, while the quantum correction still acts to stabilize the system at high wavenumbers [13].

3.3 Fractional Gravitatioanl Potential

In the framework of fractional gravity, the modified gravitational potential is defined by Eq. (1.29), and the corresponding Fourier transform is given by [12],

$$\tilde{\Phi}_s(k) = -\frac{4\pi G m \ell^{2-2s}}{k^{2s}}. \tag{2.74}$$

In three dimensions, the above expression is valid for $s < 3/2$. In this classical case, the dispersion relation is written as

$$\omega^2 = -\Omega_J^2 (\ell k)^{2-2s} + c_s^2\, k^2. \tag{2.75}$$

For this potential, the Jeans wave number is

$$k_J = \ell \left(\frac{\ell \Omega_J}{c_s} \right)^{1/s} . \tag{2.76}$$

As a result, for $k > k_J$ the oscillation of perturbation behaves as $\sim \exp(-i\omega_r t)$,with a real frequency

$$\omega_r = \sqrt{c_s^2 k^2 - \Omega_J^2 (\ell k)^{2-2s}}. \tag{2.77}$$

Conversely, for $k < k_J$, the growth rate of pertubation is written as

$$\gamma = \sqrt{\Omega_J^2 (\ell k)^{2-2s} - c_s^2 k^2}. \tag{2.78}$$

The author in the paper [12] shows the growth rate reaches its peak at $k = 0$ (corresponding to infinite wavelengths), as in Newtonian gravity. In contrast to Newtonian gravity, where the maximum growth rate is $\sqrt{4\pi G \rho_0}$, in fractional gravity, the growth rate increases as s moves away from unity and diverges in the infinite wavelength limit ($k \to 0$). In the quantum regime, the dispersion relation for the fractional gravitational potential is modified as follows [12],

$$\omega'^2 = -\Omega_J^2 \, (\ell k)^{2-2s} + \frac{\hbar^2 k^4}{4m^2} . \tag{2.79}$$

The growth rate of unstable modes is then expressed as:

$$\gamma' = \sqrt{\Omega_J^2 \, (\ell k)^{2-2s} - \frac{\hbar^2 k^4}{4m^2}}. \tag{2.80}$$

In this case, the behavior of the instability depends on the fractional parameter s, while the quantum term continues to suppress short-wavelength perturbations [12]. Among the different cases considered, the dispersion relation in an expanding background has been explicitly derived only within the framework of fractional gravity, for which it takes the form:

$$\ddot{\delta} + 2\frac{\dot{a}_{\mathrm{s}}}{a_{\mathrm{s}}}\dot{\delta} + \left(\frac{c_s^2 k^2}{a_{\mathrm{s}}^2} - \Omega_J^2 \left(\frac{k}{a_{\mathrm{s}}} \right)^{2-2s} \right) \delta = 0. \tag{2.81}$$

3.4 Modified Newton dynamics (MOND) $s = 3/2$

For the particular case of $s = \frac{3}{2}$, the fractional gravitational potential reduces to a logarithmic form, as shown in Eq. (1.35). The Fourier transform of the logarithmic potential in three dimensions is given by [38],

$$\mathcal{F}\{\ln(r/\ell)\} = -\frac{2\pi^2}{k^3}, \tag{2.82}$$

which leads to the Fourier transform of the potential

$$\tilde{\Phi}(k) = -\frac{4\pi GM}{\ell k^3}. \tag{2.83}$$

Using this result in the linear perturbation analysis of a selfgravitating fluid, the dispersion relation becomes [38],

$$\omega^2 = c_s^2 k^2 - \frac{\Omega_J^2}{\ell k}. \tag{2.84}$$

The Jeans wave number is obtained from the condition $\omega^2 = 0$, which yields

$$k_J = \left(\frac{\Omega_J^2}{c_s^2 \ell}\right)^{1/3}. \tag{2.85}$$

w For $k > k_J$, the perturbations oscillate with a real frequency

$$\omega_r = \sqrt{c_s^2 k^2 - \frac{\Omega_J^2}{\ell k}}. \tag{2.86}$$

Conversely, for $k < k_J$, the perturbations grow exponentially with a growth rate [38]

$$\omega_= \sqrt{\frac{\Omega_J^2}{\ell k} - c_s^2 k^2}. \tag{2.87}$$

Extending the analysis to the quantum regime, the dispersion relation takes the form[38]:

$$\omega'^2 = -\frac{\Omega_J^2}{\ell k} + \frac{\hbar^2 k^4}{4m^2}. \tag{2.88}$$

The growth rate of perturbations is then given by:

$$\gamma' = \sqrt{\frac{\Omega_J^2}{\ell k} - \frac{\hbar^2 k^4}{4m^2}}. \tag{2.89}$$

The table below provides, within the classical Newtonian framework, a comparative summary of the dispersion relations and growth rates associated with different gravitational potentials, emphasizing their role in gravitational instability.

Potential	**Dispersion Relation** ω^2	**Growth Rate** γ	**Compared with Newtonian gravity**
Newtonian	$\omega^2 = c_s^2 k^2 - 4\pi G\rho_0$	$\gamma = \sqrt{\Omega_J^2 - c_s^2 k^2}$	Reference timescale
Plummer	$\omega^2 = -\Omega_J^2\, kr_0 K_1(r_0 k) + c_s^2 k^2$	$\gamma = \sqrt{\Omega_J^2\, kr_0 K_1(r_0 k) - c_s^2 k^2}$	Slower than Newtonian
Fractional ($1 \leq s < \frac{3}{2}$)	$\omega^2 = -\Omega_J^2 (\ell k)^{2-2s} + c_s^2 k^2$	$\gamma = \sqrt{\Omega_J^2 (\ell k)^{2-2s} - c_s^2 k^2}$	Faster or slower than Newtonian Depends on s
MOND ($s = \frac{3}{2}$)	$\omega^2 \sim -\frac{\Omega_J^2}{\ell k} + c_s^2 k^2$	$\gamma = \sqrt{\frac{4\pi G\rho_0}{\ell k} - c_s^2 k^2}$	Faster than Newtonian

Table 2.1: Comparison of dispersion relations,growth rate for different gravitational potentials in the classical regime

The following table summarizes the results in the quantum regime.

Potential	**Quantum Dispersion Relation** ω^2	**Growth Rate** γ	**Effect of Quantum Term**
Newtonian (Quantum)	$\omega'^2 = -4\pi G\rho_0 + \frac{\hbar^2 k^4}{4m^2}$	$\gamma' = \sqrt{4\pi G\rho_0 - \frac{\hbar^2 k^4}{4m^2}}$	Reference case
Fractional (Quantum)	$\omega'^2 = -4\pi G\rho_0 (\ell k)^{2-2s} + \frac{\hbar^2 k^4}{4m^2}$	$\gamma' = \sqrt{4\pi G\rho_0 (\ell k)^{2-2s} - \frac{\hbar^2 k^4}{4m^2}}$	Slower collapse than Newtonian
Plummer (Quantum)	$\omega'^2 = -4\pi G\rho_0\, kr_0 K_1(kr_0) + \frac{\hbar^2 k^4}{4m^2}$	$\gamma' = \sqrt{4\pi G\rho_0\, kr_0 K_1(kr_0) - \frac{\hbar^2 k^4}{4m^2}}$	Faster or slower than Newtonian depending on s
MOND (Quantum)	$\omega'^2 = -\frac{4\pi G\rho_0}{\ell k} + \frac{\hbar^2 k^4}{4m^2}$	$\gamma' = \sqrt{\frac{4\pi G\rho_0}{\ell k} - \frac{\hbar^2 k^4}{4m^2}}$	Faster collapse than Newtonian (especially at large scales)

Table 2.2: Quantum-corrected dispersion relations and growth rates for different gravitational potentials in the Quantum regime.

4 Conclusion

In this chapter, we have undertaken a systematic investigation of Jeans instability through a linear perturbative treatment of the hydrodynamic equations coupled self-consistently to Poissons equation. By introducing small fluctuations around a homogeneous background and decomposing them into Fourier modes, we derived the dispersion relation that governs the dynamical stability of a self-gravitating medium. The analysis reveals a sharp scale-dependent behavior: perturbations with wavenumbers exceeding the Jeans critical threshold remain dynamically stable and propagate as oscillatory sound-like modes, whereas long-wavelength perturbations below this critical scale undergo exponential amplification, signaling the onset of gravitational collapse. This delineation between stability and instability highlights the fundamental role of pressuregravity competition in structure formation.

Moreover, as established in previous studies, modifications to the gravitational potential systematically affect both the critical Jeans wavenumber and the corresponding growth rate of unstable modes. These modifications indicate that even slight departures from standard gravitational theory can significantly alter the characteristic mass scale and collapse timescale of self-gravitating systems, thereby potentially imprinting observable signatures on the formation and evolution of cosmic structures.

Chapter 3

Probing Gravitational Instability for Hernquist Potential

1 Introduction

The classical Newtonian gravitational potential,

$$\Phi(r) \sim -\frac{1}{r}, \tag{3.1}$$

provides the standard framework for describing gravitational interactions in self-gravitating systems. Despite its remarkable success, the $1/r$ behavior leads to a mathematical singularity in the limit $r \to 0$, which complicates analytical treatments and may produce artificial close encounters in N-body simulations. These numerical effects can affect the realistic modeling of extended astrophysical systems such as galaxies and dark matter halos.

To overcome these limitations, several regularized gravitational potentials have been proposed that preserve the Newtonian behavior at large distances while smoothing the interaction at small scales. Among them, the Hernquist gravitational potential is given by

$$\Phi(r) = -\frac{GM}{r+a}, \tag{3.2}$$

where a is a characteristic structural (softening) length scale associated with the finite spatial extent of the mass distribution. Originally introduced to reproduce the surface brightness profiles of elliptical galaxies, the Hernquist model provides a simple and analytically tractable description of the gravitational field of spherical stellar systems [39]. Because of these properties, it has become a widely used potential in studies of galactic dynamics and astrophysical structure modeling.

In this chapter, we study Jeans instability within the context of the Hernquist potential (3.2), and see how the scale radius affects the gravitational instability. Studying Jeans analysis for Hernquist potential is important because it links the systems internal mass distribution to its dynamical properties. This approach provides a quantitative way to evaluate the stored energy and understand how the internal structure affects the systems response to perturbations.

2 Jeans Mass and Radius for the Hernquist Model

To analyze the Jeans instability, we first consider the gravitational binding energy U, defined as

$$U = -\int_0^M |\Phi| \, dm, \tag{3.3}$$

where Φ is given by Eq. (3.2). For a spherical cloud of radius R with uniform density ρ and total mass M, the enclosed mass and differential mass element are

$$m(r) = \frac{4\pi}{3}\rho r^3 \quad \Rightarrow \quad dm = 4\pi\rho r^2 dr, \tag{3.4}$$

$$M = \frac{4\pi}{3}\rho R^3. \tag{3.5}$$

Using Eqs. (3.3), (3.4), and (3.5), the gravitational binding energy can be written as

$$U = -\int_0^R \frac{16\pi^2 G\rho^2}{3} \frac{r^5}{r+a} \, dr. \tag{3.6}$$

This integral has a closed-form solution:

$$U = -\frac{16\pi^2\rho^2 G}{3}\left[a^4 R - \frac{a^3R^2}{2} + \frac{a^2R^3}{3} - \frac{aR^4}{4} + \frac{R^5}{5} + a^5 \ln\left(\frac{a}{a+R}\right)\right]. \tag{3.7}$$

Since the binding energy must be negative, it is instructive to examine the range of a in terms of R that satisfies this condition. Writing Eq. (3.7) in terms of $x = R/a$, we have

$$U = -\frac{16\pi^2 R^5\rho^2 G}{3}\left[\frac{1}{x^4} - \frac{1}{2x^3} + \frac{1}{3x^2} - \frac{1}{x} + \frac{1}{5} + \frac{1}{x^5}\ln(1+x)\right]. \tag{3.8}$$

For the binding energy to be negative, the terms inside the brackets must satisfy

$$\frac{1}{x^4} - \frac{1}{2x^3} + \frac{1}{3x^2} - \frac{1}{x} + \frac{1}{5} + \frac{1}{x^5}\ln(1+x) > 0. \tag{3.9}$$

Numerical solution of this inequality yields two positive intervals: $0 < x < 1.27662$ and $x > 4.962$, corresponding to the constraints

$$R < 1.27662\, a, \tag{3.10}$$

$$R > 4.962\, a. \tag{3.11}$$

As the Jeans analysis focuses on large-scale structures, we consider the latter case, adopting for simplicity

$$R \geq 5a. \tag{3.12}$$

Using Eq. (3.5), the gravitational binding energy can then be rewritten as

$$U = -\frac{3GM^2}{R}\left[\frac{1}{x^4} - \frac{1}{2x^3} + \frac{1}{3x^2} - \frac{1}{x} + \frac{1}{5} + \frac{1}{x^5}\ln(1+x)\right]. \tag{3.13}$$

In the limit $a \to 0$ (or $x \to \infty$), this expression reduces to the standard Newtonian result $U = -3GM^2/(5R)$. Since the Hernquist potential complicates an exact analytical computation of R_J, we exploit the approximation $R \geq 5a$ ($R/a \gg 1$), retaining only the dominant term $1/x$ and neglecting higher-order contributions. This leads to the quadratic equation for $y = R_J/a$, the gravitational potential energy reduces to

$$U \simeq -\frac{16\pi^2 G\rho^2 a^5}{3}\left(\frac{1}{y} - \frac{1}{5}\right), \tag{3.14}$$

whereas the thermal kinetic energy is given by

$$K = \frac{3Mk_BT}{2m_p\mu}, \qquad M = \frac{4}{3}\pi\rho(ya)^3. \tag{3.15}$$

By enforcing the Jeans instability criterion,

$$K = |U|. \tag{3.16}$$

We obtain a quadratic equation in y

$$\frac{Ay^2}{5} - Ay - B = 0, \tag{3.17}$$

where

$$A = \frac{16\pi^2\rho^2 a^5 G}{3}, \quad B = \frac{2\pi\rho a^3 k_B T}{m_p \mu}. \tag{3.18}$$

The discriminant is positive, $\Delta = A^2 + \frac{4AB}{5}$, giving two solutions:

$$y_1 = \frac{5}{2}\left(1 + \sqrt{1 + \frac{4B}{A}}\right), \quad y_2 = \frac{5}{2}\left(1 - \sqrt{1 + \frac{4B}{A}}\right). \tag{3.19}$$

Only y_1 is physically meaningful because it ensures a positive value for the Jeans radius. Hence, the Jeans radius for the Hernquist potential is

$$R_J^{(a)} = \frac{5}{2}\left[a + \sqrt{a^2 + \frac{3k_B T}{10\pi\rho m_p \mu G}}\right], \tag{3.20}$$

and the corresponding Jeans mass is

$$M_J^{(a)} = \frac{125\pi}{6}\rho\left[a + \sqrt{a^2 + \frac{3k_B T}{10\pi\rho m_p \mu G}}\right]^3. \tag{3.21}$$

In the Newtonian limit ($a \to 0$), one recovers the classical expressions:

$$R_J^{(a=0)} = \sqrt{\frac{15k_B T}{8\pi\rho m_p \mu G}}, \quad M_J^{(a=0)} = \frac{4\pi\rho}{3}\left(\frac{15k_B T}{8\pi\rho m_p \mu G}\right)^{3/2}. \tag{3.22}$$

which is consistent with the standard Newtonian Jeans expressions derived in Chapter 1 (see Eqs (1.15) and (1.16). This agreement confirms that, in the limit $a \to 0$, the Hernquist potential naturally recovers the classical Newtonian gravitational behavior.

It is evident that a finite scale parameter a increases both the Jeans radius and mass, indicating that the critical mass for gravitational collapse is raised. This mechanism may account for the stability of interstellar clouds whose masses exceed the classical Jeans mass yet avoid collapse. The parameter a can also be tuned to achieve consistency with observational data. For example, the dense molecular cloud core Oph-2 remains starless despite having a mass $M \simeq 2.05M_J$ and shows no embedded protostar or infrared emission [40]. This observation allows us to constrain a such that the Hernquist-modified Jeans mass exceeds the cloud's mass:

$$M_J^{(a)} > 2.05 M_J. \tag{3.23}$$

Given Oph-2's central temperature $T = 7\,\mathrm{K}$ and number density $n = 1.2 \times 10^6\,\mathrm{cm}^{-3}$ [41], the inequality (3.23) yields

$$a > 2.45 \times 10^{13}\,\mathrm{m} \simeq 7.9 \times 10^{-4}\,\mathrm{pc} \simeq 164\,\mathrm{AU}. \tag{3.24}$$

At this stage, it is important to compare the constraint imposed on a (inequality (3.24)) with some estimated values of the same parameter in order to ensure consistency with observational data. For instance, in Ref. [42], the parameter a was estimated to be of the order of $16.9 \pm 2.3\,\mathrm{kpc}$ so as to be consistent with the kinematic data of the Milky Way. This estimate is fully consistent with the constraint (3.24). In addition, The researchers in the paper [43] measured the stellar density in the smooth halo of the Andromeda galaxy using photometric images, i.e., determining the number of stars per unit area at different distances from the galaxy's center. They then applied the Hernquist model to these data, choosing the *scale radius* a so that the density profile of the model would best match the observed data. The results show that $a \approx 17$ kpc provides the best agreement between the observed stellar density in the smooth halo and the theoretical model, making this model suitable for describing the distribution of stars in the halo. This is also constinent with the constraint (3.23).

3 Dispersion Relations in Hernquist Potential

3.1 Classical Regime

In the following analysis, we adopt the Hernquist gravitational kernel ,

$$V(r) = -\frac{G}{r+a}, \tag{3.25}$$

which provides a regularized description of the gravitational field at short distances.

The fourier transforml of Hernquist potential gives

$$\tilde{V}(k) = -4\pi G M \int_0^{+\infty} dr \frac{r^2}{r+a} \frac{\sin(kr)}{kr}. \tag{3.26}$$

This integral does not converge, so, we will introduce exponential factor $\exp(-\varepsilon r)$, then take $\varepsilon \to 0^+$. Under this method, one gets

$$\tilde{V}(k) = -\frac{4\pi G}{k} \lim_{\varepsilon \to 0^+} \int_0^{+\infty} dr \frac{r^2}{r+a} \frac{\sin(kr)}{r} \exp(-\varepsilon r). \tag{3.27}$$

This integral has closed form, which is given by

$$\tilde{V}(k) = -\frac{4\pi G}{k^2} \left(1 - \frac{a\pi \cos(ak)}{k} + \frac{ia}{2k} \left[exp(iak)\,\mathrm{Ei}(-iak) - exp(-iak)\,\mathrm{Ei}(iak)\right]\right) \tag{3.28}$$

Using the identity ([44], Section 8.233)

$$\mathrm{Ei}(\pm ix) = \mathrm{Ci}(x) \pm i\,\mathrm{Si}(x) \tag{3.29}$$

one gets more simplified form

$$\tilde{V}(k) = -\frac{4\pi G}{k^2} \left[1 - \frac{a\pi \cos(ak)}{k} + \frac{a}{k} \left(\sin(ak)\,\mathrm{ci}(ak) - \cos(ak)\,\mathrm{si}(ak)\right)\right]. \tag{3.30}$$

As a result, the dispersion relation for this system is written as

$$\omega^2 = -\Omega_J^2 \left[1 - ak\pi \cos(ak) + ak\Big(\sin(ak)\,\mathrm{ci}(ak) - \cos(ak)\,\mathrm{si}(ak)\Big)\right] + c_s^2 k^2. \tag{3.31}$$

In the limit $a = 0$, the usual dispersion relation is recovered

$$\omega_{a=0}^2 = -\Omega_J^2 + c_s^2 k^2. \tag{3.32}$$

By introducing appropriate dimensionless quantities, the dispersion relation in Eq. (2.38) takes the form

$$\mathcal{W}^2 = K\Upsilon\pi \cos(K\Upsilon) - K\Upsilon\Big(\sin(K\Upsilon)\,\mathrm{ci}(K\Upsilon) - \cos(K\Upsilon)\,\mathrm{si}(K\Upsilon)\Big) - 1 + K^2. \tag{3.33}$$

where $\mathcal{W} = \omega/\Omega_J, K = c_s k/\Omega_J, \Upsilon = a\Omega_J/c_s$. As seen from Eq. (3.33), for sufficiently large K (i.e., at high wave numbers), the contribution of the second term diminishes compared to the leading one, so that the dependence on a effectively vanishes. The instability growth rate is obtained from the imaginary component of ω and, when rendered dimensionless, is defined as $\Gamma = \mathrm{Im}(\omega)/\Omega_J$. For Hernquist gravitational potential, the dimensionless growth rate is given as

$$\Gamma = \sqrt{K\Upsilon\left(\sin(K\Upsilon)\,\mathrm{ci}(K\Upsilon) - \cos(K\Upsilon)\,\mathrm{si}(K\Upsilon)\right) - K\Upsilon\pi\cos(K\Upsilon) + 1 - K^2}. \qquad (3.34)$$

The variations of growth rate under the impact of a is presented in Fig. 3.1.

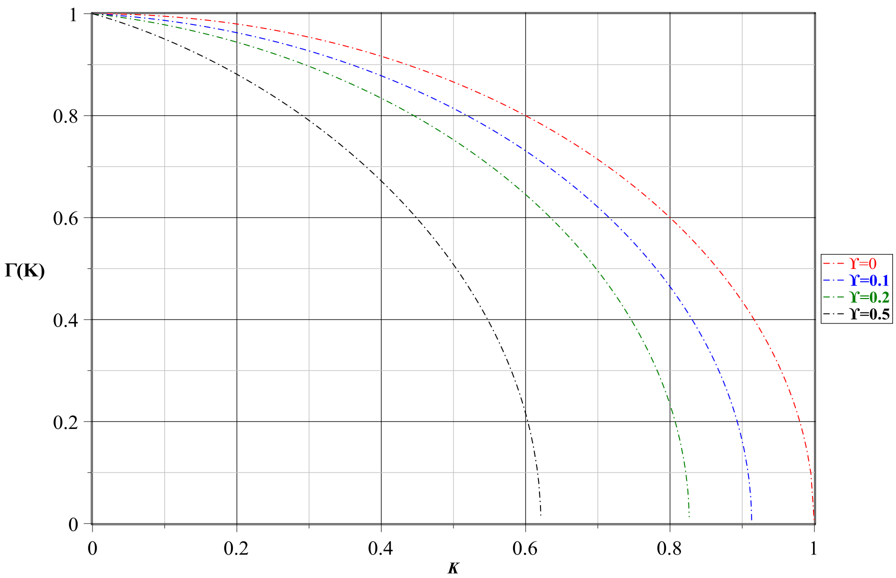

Figure 3.1: Dimensionless growth rate for a Hernquist potential as a function of $K = c_s k/\Omega_J$ for different values of $\Upsilon = a\Omega_J/c_s$. Here, Ω_J is the Jeans frequency, c_s the sound speed, and a the scale length.

The Hernquist potential yields a suppressed growth rate compared to the standard Newtonian case. In the long-wavelength limit ($k \to 0$), both models attain the same maximum growth rate. However, the introduction of the scale radius a shifts the cutoff wavenumberat which the growth rate vanishestoward smaller values. This means that the Jeans wavenumber decreases (and the Jeans wavelength grows) as the scale radius effect increases. This behavior contrasts with that found for the Maneff, logarithmic, and Yukawa potentials studied in Ref. [38], where gravitational instability sets in at shorter wavelengths, but is consistent with the trend observed for the Plummer sphere profile [13]. Taken together, these results indicate that incorporating a promotes the development of gravitational instability on larger spatial scales relative to the pure Newtonian case.

The dispersion relation for the Hernquist potential in an expanding universe is given by:

$$\ddot{\delta} + 2\frac{\dot{a}_s}{a_s}\dot{\delta} + \left[\frac{c_s^2 k^2}{a_s^2} - \frac{4\pi G\rho_0}{m}\left(1 - \frac{a\pi a_s}{k}\cos\left(\frac{ak}{a_s}\right)\right.\right.$$
$$\left.\left.+\frac{aa_s}{k}\left(\sin\left(\frac{ak}{a_s}\right)\mathrm{ci}\left(\frac{ak}{a_s}\right) - \cos\left(\frac{ak}{a_s}\right)\mathrm{si}\left(\frac{ak}{a_s}\right)\right)\right)\right]\delta = 0 \tag{3.35}$$

3.2 Quantum Regime

For the Hernquist potential, the quantum version of the dispersion relation is simply given by

$$\omega^2 = -\Omega_J^2\left[1 - ak\pi\cos(ak) + ak\Big(\sin(ak)\,\mathrm{ci}(ak) - \cos(ak)\,\mathrm{si}(ak)\Big)\right] + \frac{\hbar^2 k^4}{4m^2}. \tag{3.36}$$

For small wave number $k \to 0$, one can neglect the terms with k^2 or more, therefore, one gets

$$\omega^2_{\text{small }k} \simeq -\Omega_J^2\left[1 - ak\pi + a^2k^2\ln(ak)\right] \tag{3.37}$$

For sufficiently small ak (or in the long-wavelength regime $a << \lambda$), the squared frequency ω^2 remains negative, indicating that the system is unstable for all long-wavelength modes. However, the presence of the characteristic scale a softens the gravitational instability.

On the other hand, for small wavlngth mode $ak >> 1$ (or equivantely $a >> \lambda$), one gets

$$\omega^2_{\text{large-wave number}} \simeq -\Omega_J^2\Big(2 - ak\pi\cos(ak)\Big) + \frac{\hbar^2 k^4}{4m^2}. \tag{3.38}$$

In this case, In the quantum regime, the growth rate can be expressed in dimensionless form as

$$\Gamma = \sqrt{\varrho\vartheta\Big(\sin(\varrho\vartheta)\,\mathrm{ci}(\varrho\vartheta) - \cos(\varrho\vartheta)\,\mathrm{si}(\varrho\vartheta)\Big) - \varrho\vartheta\pi\cos(\varrho\vartheta) + 1 - \varrho^4}. \tag{3.39}$$

Here, the dimensionless parameters ϑ and ϱ are defined as $\vartheta = a\sqrt{\frac{2m\Omega_J}{\hbar}}, \varrho = \sqrt{\frac{\hbar}{2m\Omega_J}}k$. Physically, they present represents the position a scaled by the quantum characteristic length $\ell_0 = \sqrt{\hbar/(2m\Omega_J)}$, indicating displacement relative to the natural quantum scale, and represents the wave number scaled by the same quantum length, giving the dimensionless phase or oscillation of the wave, respectively.

4 Conclusion

In this chapter, we investigated the gravitational instability of a self-gravitating system within the Hernquist potential framework, adopted as a suitable model for centrally concentrated structures such as molecular clouds and galaxies. We showed that the introduction of the scale length a significantly modifies the instability criteria, leading to an increase in both the Jeans radius and Jeans mass compared to the Newtonian case. This highlights the crucial role of internal structure in determining gravitational collapse. Application to the Oph-2 cloud demonstrated that appropriate values of a can account for its observed stability despite exceeding the classical Jeans mass, emphasizing the relevance of the Hernquist potential in connecting theory with observations. Moreover, the obtained values of a are consistent with independent estimates from galaxy studies. The dispersion relation analysis further revealed that the scale length suppresses the growth of perturbations and shifts the instability threshold toward larger wavelengths. In the quantum regime, the Bohm pressure introduces an additional stabilization at small scales. Overall, this chapter demonstrates that incorporating a scale length in the gravitational potential provides a flexible framework for studying stability in both classical and quantum systems. Possible extensions include the effects of rotation, magnetic fields, and relativistic corrections, as well as applications to dark matter models and early-universe structure formation.

General Conclusion

In this work, we carried out a comprehensive study of gravitational instability within the framework of Jeans analysis by combining the energetic approach and dynamical analysis, and applying them to several models of gravitational potentials, including the Newtonian case and modified gravity models, with particular focus on the Hernquist potential. The results showed that the nature of the gravitational potential plays a crucial role in determining the conditions for collapse. Modifications to the form of the potential lead to significant changes in the Jeans mass and length, and consequently in the properties of structure formation. The dynamical analysis also revealed that system stability strongly depends on the wavelength, where large-scale perturbations grow while small-scale perturbations remain stable or oscillatory. Furthermore, the study in the quantum regime highlighted that quantum pressure provides an additional mechanism to resist collapse, especially at small scales, emphasizing the complex interplay between gravity and quantum effects. In the case of the Hernquist potential, introducing a characteristic scale length leads to an increase in the Jeans mass and delays collapse, which helps explain the stability of certain astrophysical systems beyond classical limits. Overall, this study confirms that Jeans analysis remains a powerful and flexible tool for understanding the dynamics of self-gravitating systems, particularly when extended to include more realistic physical effects. As for future perspectives, this work can be extended by:

- Including the effects of rotation and magnetic fields on the stability of gaseous clouds [45, 46].
- Investigating general relativity effects in high-density systems [47].
- Applying the results to ultra-light dark matter models [48].
- And studying gravitational instability in an expanding universe with more accurate connections to modern cosmological observations [49].
- Gravitational Instability in the Collisionless Boltzmann Framework [50].

- Extending the Jeans analysis to dusty plasmas takes into account electrostatic interactions, leading to a modification of the classical criterion by introducing the contribution of the electrostatic potential alongside gravity, thereby altering the instability conditions through the competition between gravitational andelectrostatic effects [51, 52, 53].

Bibliography

[1] James Jeans. The stability of a spherical nebula. *Philosophical Transactions of the Royal Society of London A*, 199:1–53, 1902.

[2] P. J. E. Peebles. *Principles of Physical Cosmology*. Princeton University Press, 1993.

[3] James Binney and Scott Tremaine. *Galactic Dynamics*. Princeton University Press, 2nd edition, 2008.

[4] Frank H. Shu. *The Physics of Astrophysics: Gas Dynamics*. University Science Books, 1992.

[5] T. Padmanabhan. *Structure Formation in the Universe*. Cambridge University Press, 1993.

[6] Bruce G. Elmegreen. Star formation from galaxies to globules. *The Astrophysical Journal*, 577:206–220, 2002.

[7] Christopher F. McKee and Eve C. Ostriker. Theory of star formation. *Annual Review of Astronomy and Astrophysics*, 45:565–687, 2007.

[8] Steven A. Balbus and John F. Hawley. Magnetohydrodynamic stability of accretion disks. *The Astrophysical Journal*, 376:214–233, 1991.

[9] Ralf S. Klessen and Simon C. O. Glover. Star formation in molecular clouds. *Annual Review of Astronomy and Astrophysics*, 54:105–145, 2016.

[10] Salvatore Capozziello and Mariafelicia De Laurentis. Extended theories of gravity. *Physics Reports*, 509:167–321, 2011.

[11] Benoit Famaey and Stacy S. McGaugh. Modified newtonian dynamics (mond): Observational phenomenology and relativistic extensions. *Living Reviews in Relativity*, 15(10), 2012.

[12] Kamel Ourabah. Jeans analysis in fractional gravity. *The European Physical Journal C*, 84(10):1047, 2024.

[13] Abdelhakim Benkrane. Gravitational instability in plummer sphere profile: A jeans analysis. *New Astronomy*, page 102493, 2025.

[14] Houjun Mo, Frank C. van den Bosch, and Simon White. *Galaxy Formation and Evolution*. Cambridge University Press, 2010.

[15] Henry Crozier Plummer. On the problem of distribution in globular star clusters. *Monthly Notices of the Royal Astronomical Society*, 71:460–470, 1911.

[16] Farooq Ahmad, William C. Saslaw, and Naseer Iqbal Bhat. Statistical mechanics of the cosmological many-body problem. *The Astrophysical Journal*, 571(2):576, 2002.

[17] Volker Springel. The cosmological simulation code gadget-2. *Monthly Notices of the Royal Astronomical Society*, 364(4):1105–1134, 2005.

[18] David Merritt. Optimal smoothing for n-body codes. *The Astronomical Journal*, 111:2462, 1996.

[19] Walter Dehnen. N-body simulations of disc galaxies: optimal softening and adaptive force calculation. *Monthly Notices of the Royal Astronomical Society*, 414(4):2005–2015, 2011.

[20] Andrea Giusti. Mond-like fractional laplacian theory. *Physical Review D*, 101:124029, 2020.

[21] Abdelhakim Benkrane. Jeans mechanism in the context of modified newtonian dynamics. *European Physical Journal Plus*, 140(6):499, 2025.

[22] S. Chandrasekhar. *Hydrodynamic and Hydromagnetic Stability*. Oxford University Press, 1961.

[23] J. H. Jeans. Stability of gaseous spheres. *Philosophical Transactions of the Royal Society A*, 1919.

[24] P. Ledoux. The stability of gaseous stars. *Astrophysical Journal*, 1951.

[25] Pierre-Henri Chavanis. Jeans instability. *Astronomy & Astrophysics*, 483:673–685, 2011.

[26] L. Spitzer. *Diffuse Matter in Space*. Wiley, 1968.

[27] R. B. Larson. Numerical calculations of the dynamics of a collapsing proto-star. *Monthly Notices of the Royal Astronomical Society*, 1969.

[28] P. Goldreich and S. V. Lynden-Bell. Gravitational stability of uniformly rotating disks. *Monthly Notices of the Royal Astronomical Society*, 1965.

[29] S. Chandrasekhar. *Ellipsoidal Figures of Equilibrium.* Yale University Press, 1969.

[30] Gilberto M. Kremer. Jeans instability from post-newtonian boltzmann equation. *The European Physical Journal C*, 81:927, 2021.

[31] Kamel Ourabah. *Collective Phenomena in Plasmas and Elsewhere: Kinetic and Hydrodynamic Approaches.* Springer, 2018.

[32] Bradley W. Carroll and Dale A. Ostlie. *An Introduction to Modern Astrophysics.* Pearson, 2nd edition, 2007.

[33] W. B. Bonnor. Boyle's law and gravitational instability. *Monthly Notices of the Royal Astronomical Society*, 117:104–117, 1957.

[34] Remo Ruffini and Silvano Bonazzola. Systems of self-gravitating particles in general relativity and the concept of an equation of state. *Physical Review*, 187(5):1767, 1969.

[35] L. Diósi. Gravitation and quantum-mechanical localization of macro-objects. *Physics Letters A*, 105(4):199–202, 1984.

[36] Roger Penrose. On gravity's role in quantum state reduction. *General relativity and gravitation*, 28(5):581–600, 1996.

[37] Erwin Madelung. Quantum theory in hydrodynamical form. *z. Phys*, 40:322, 1927.

[38] Ryan Khaled and Kamel Ourabah. Jeans analysis in modified gravity: a general formulation. *The European Physical Journal C*, 85(12):1482, 2025.

[39] L. Hernquist. An analytical model for spherical galaxies and bulges. *The Astrophysical Journal*, 356:359–364, 1990.

[40] Sarah I Sadavoy, James Di Francesco, and Doug Johnstone. starless super-jeans cores in four gould belt clouds. *The Astrophysical Journal Letters*, 718(1):L32–L37, 2010.

[41] Dimitris Stamatellos, Anthony P Whitworth, and Derek Ward-Thompson. The dust temperatures of the pre-stellar cores in the ρ oph main cloud and in other star-forming regions: consequences for the core mass function. *Monthly Notices of the Royal Astronomical Society*, 379(4):1390–1400, 2007.

[42] Gwendolyn M Eadie, William E Harris, and Lawrence M Widrow. Estimating the galactic mass profile in the presence of incomplete data. *The Astrophysical Journal*, 806(1):54, 2015.

[43] Mikito Tanaka, Masashi Chiba, Yutaka Komiyama, Puragra Guhathakurta, Jason S Kalirai, and Masanori Iye. Structure and population of the andromeda stellar halo from a subaru/suprime-cam survey. *The Astrophysical Journal*, 708(2):1168, 2009.

[44] Izrail Solomonovich Gradshteyn and Iosif Moiseevich Ryzhik. *Table of integrals, series, and products*. Academic press, 2014.

[45] R. C. Sharma. The thermal-convective instability in a stellar atmosphere with rotation and hall effects. *Zeitschrift für Naturforschung A*, 29:867–869, 1974.

[46] M. K. Vyas and R. K. Chhajlani. Magnetogravitational instability of a thermally conducting rotating plasma through a porous medium. *Contributions to Plasma Physics*, 29(1):91–108, 1989.

[47] A. A. Jackson. Relativistic hydrodynamics and gravitational instability revisited. *Monthly Notices of the Royal Astronomical Society*, 264:729–746, 1993.

[48] Elisa G. M. Ferreira. Ultra-light dark matter. *The Astronomy and Astrophysics Review*, 29(1):7, 2021.

[49] Peter Anninos. Computational cosmology: From the early universe to the large scale structure. *Living Reviews in Relativity*, 1(9), 1998.

[50] D. Lynden-Bell. Statistical mechanics of violent relaxation in stellar systems. *Monthly Notices of the Royal Astronomical Society*, 136:101–121, 1967.

[51] B. P. Pandey, K. Avinash, and C. B. Dwivedi. Jeans instability in dusty plasma. *Physical Review E*, 49:5599, 1994.

[52] F. Verheest, P. K. Shukla, G. Jacobs, and V. V. Yaroshenko. Gravitational instability in dusty plasmas. *Physical Review E*, 68:027402, 2003.

[53] G. L. Delzanno, G. Lapenta, and M. Rosenberg. Modified jeans instability with nonmonotonic potentials. *Physical Review Letters*, 94:175005, 2005.